Respiratory Medicine Case Reports 49 (2024) 102020

Contents lists available at ScienceDirect

Respiratory Medicine Case Reports

journal homepage: www.elsevier.com/locate/rmcr

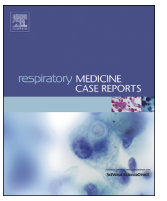

Case Report

Barking up the wrong tree: Vascular tree-in-bud due to intravascular lymphoma

Ravi Manglani [a, *], Ji-Hae Shin [b], Venkata Sireesha Chemarthi [b], Mohamad Raji [c], Anna Rozenshtein [d], Oleg Epelbaum [a]

[a] Division of Pulmonary, Critical Care and Sleep Medicine, Westchester Medical Center, New York Medical College, Valhalla, NY, USA
[b] Department of Medicine, Lincoln Medical Center, Bronx, NY, USA
[c] Department of Pathology, Lincoln Medical Center, Bronx, NY, USA
[d] Department of Radiology, Section of Cardiac and Thoracic Imaging, Westchester Medical Center Health Network, Valhalla, NY, USA

ARTICLE INFO

Handling Editor: AC Amit Chopra

Keywords:
Fever of unknown origin
Intravascular lymphoma
Lung nodules

ABSTRACT

A 59-year-old previously healthy woman presented with a six-month history of fever, nonproductive cough, and weight loss. The cause of these symptoms remained obscure despite a thorough, month-long hospitalization. On presentation, she was normotensive with a pulse of 98 beats/minute, respiratory rate of 20 breaths/minute, and a temperature of 39.4C. She was emaciated. Physical examination was notable for faint bibasilar crackles on lung auscultation. Initial laboratory testing revealed pancytopenia. Peripheral smear demonstrated normocytic, normochromic anemia without immature cells or schistocytes. Other notable laboratory findings included elevated levels of lactate dehydrogenase, elevated ferritin, and elevated levels of fasting serum triglycerides. A comprehensive laboratory evaluation for connective tissue disease was negative. Plain chest radiography was normal while computed tomography (CT) of the chest demonstrated sub-centimeter nodules in a branching centrilobular pattern as well as in a peri-lymphatic distribution without associated lymphadenopathy or organomegaly.

The above constellation of laboratory abnormalities raised concern for hemophagocytic lymphohistiocytosis (HLH). Soluble IL-2 (CD25) receptor levels were markedly elevated. Bronchoscopy with transbronchial biopsies of the right lower lobe was performed, revealing intravascular lymphoma associated with HLH. Our case emphasizes the need for clinicians to consider vascular causes of tree - in-bud nodules in addition to the conventional bronchiolar causes. The case also is a reminder of the need to conduct an exhaustive search for malignancy, in patients with HLH.

1. Case presentation

A 59-year-old woman, native of the Dominican Republic, travelled to the United States for medical evaluation and presented to our institution in New York City with a six-month history of fever, malaise, nonproductive cough, and 20-lb weight loss. The cause of these symptoms remained obscure despite a thorough, month-long evaluation in her home country. On presentation, she was normotensive with a pulse of 98 beats/minute, respiratory rate of 20 breaths/minute, and a temperature of 39.4C. She was emaciated.

Abbreviations: CT, Computed Tomography; GGO, Ground glass opacities; HLH, hemophagocytic lymphohistiocytosis; IHC, immunohistochemistry; IVBCL, intravascular large B-cell lymphoma; MIP, maximal intensity projection.

* Corresponding author. Westchester Medical Center, 100 Woods Road, Macys Pavilion, Valhalla, NY, 10595, USA.
E-mail address: drravipm@gmail.com (R. Manglani).

https://doi.org/10.1016/j.rmcr.2024.102020
Received 29 August 2022; Received in revised form 23 March 2024; Accepted 27 March 2024
Available online 5 April 2024

Physical examination was notable for faint bibasilar crackles on lung auscultation. Initial laboratory testing revealed pancytopenia: leukocyte count of 1470 cells/μL (normal range 4.5-11x 10^9 cells/L), hemoglobin 8 gm/dL (normal range 12–15.5 g/dL), and platelet count of 49,000/μL(normal range 150,000–440,000 cells/μL). Peripheral smear demonstrated normocytic, normochromic anemia without immature cells or schistocytes. Other notable laboratory findings were a lactate dehydrogenase level of 3349 units/L (normal range 140–280 Units/L), ferritin level of 8723 ng/ml (normal range 20–250 ng/ml), and fasting serum triglycerides of 751 mg/dL (normal range 50–150 mg/dL). Serological evaluation for infection, including testing for human immunodeficiency virus, cytomegalovirus, Epstein-Barr virus, 1,3-β-D-glucan, and galactomannan, was negative as were routine blood cultures. Comprehensive laboratory evaluation for connective tissue disease was likewise negative. Plain chest radiography was normal while computed tomography (CT) of the chest demonstrated sub-centimeter nodules in a branching centrilobular pattern (Fig. 1A) as well as in a perilymphatic distribution (Fig. 1B) without associated lymphad

1.1. Enopathy or organomegaly

The above constellation of laboratory abnormalities raised concern for hemophagocytic lymphohistiocytosis (HLH). Testing for soluble IL-2 (CD25) receptor revealed a level of 27,427 pg/ml (normal range 175–858 pg/ml). Bone marrow biopsy showed maturing trilineage hematopoiesis without evidence of infection, malignancy, or any other pathology. Meanwhile, sputum analysis for mycobacterial and fungal organisms returned negative. Bronchoscopy with transbronchial biopsies of the right lower lobe was performed.

2. What is the diagnosis?

Transbronchial biopsy tissue (Fig. 2) revealed the presence of large neoplastic lymphoid cells localized to the lung interstitium as well as the lumina of terminal arterioles and capillaries. Morphology and immunohistochemistry (IHC) were consistent with intravascular large B-cell lymphoma (IVLBCL) of the lung.

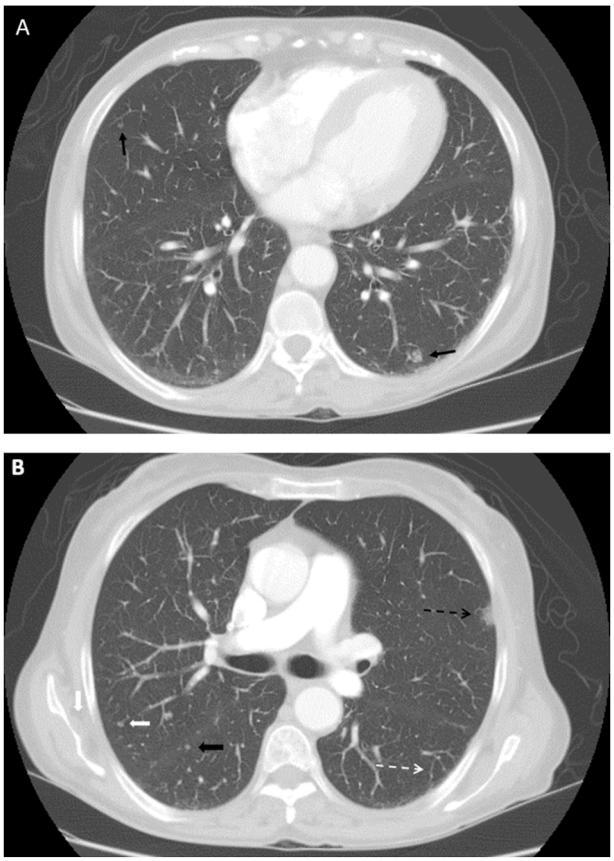

Fig. 1. A, Axial section from chest CT performed after administration of intravenous contrast material and set to lung window demonstrates branching centrilobular nodules (black arrows) following blood vessels without associated air trapping.
B, Axial section from the same chest CT as in panel A but at a more cranial level demonstrates the additional findings of nodules in a perilymphatic distributions along fissural pleura (solid black arrow) as well as focal ground glass opacity (black dashed arrow) and branching vasculature in the periphery (dashed white arrow). Further examples of centrilobular nodules with feeding blood vessels and without evidence of air trapping are likewise seen at this level (solid white arrows).

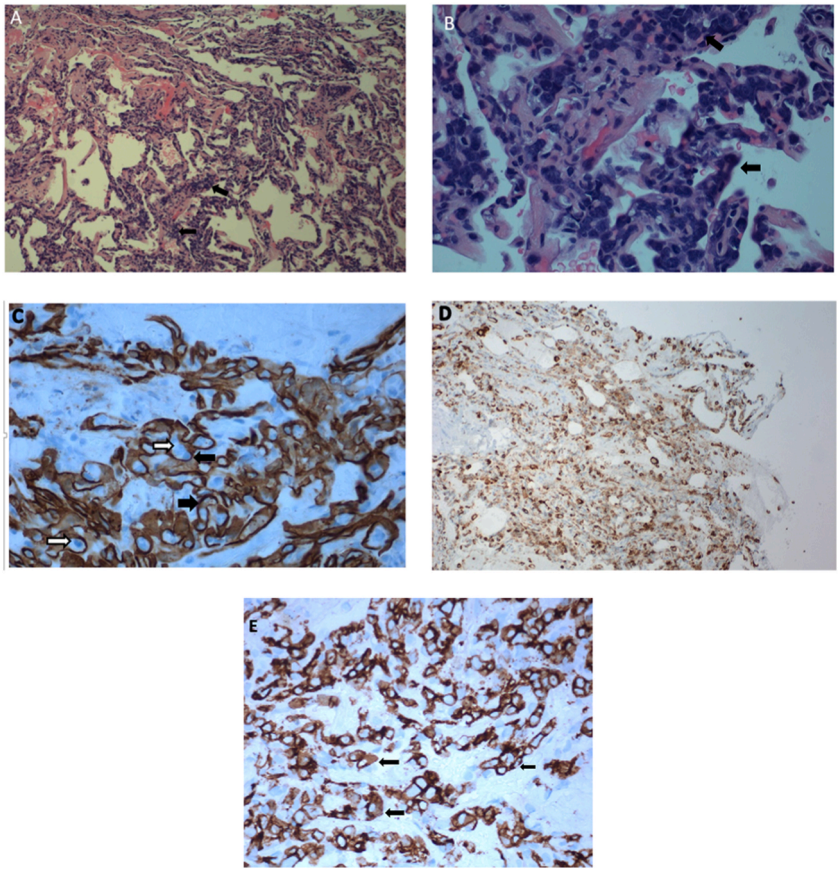

Fig. 2. A-E, Histology; A and B, Hematoxylin & Eosin stain of the transbronchial lung biopsy showing focal proliferation of large atypical lymphoid cells with prominent nucleoli (black arrows) at low power in A (original magnification 10X) and at high power in B (original magnification 100X). C, Immunohistochemical staining for CD34 contrasts positively staining endothelial cells (black arrows) with non-staining atypical lymphoid cells (white arrows) within the alveolar capillaries and small blood vessels (original magnification 100X). D and E, Immunohistochemical staining for CD20 identifies B lymphocytes (black arrows in panel E) distributed within the interstitial and vascular compartments of the lung, (Panel D low power, original magnification 10X; Panel E original magnification 100X).

3. How does the pathology correlate with the radiological finding of branching centrilobular nodules?

The pattern of branching centrilobular nodules on chest CT refers to centrilobular nodularity with an appearance resembling the letters "V" or "Y" and typically corresponding to bronchiolar mucus impaction in the setting of endobronchial infection. However, endobrochial disease is usually associated with lucency of the surrounding lung parenchyma due to air trapping, which was absent in this case. In addition, perilymphatic distribution of nodules suggested a more complex process, such as sarcoidosis or malignancy. In this case, lobular arterioles coursing in the center of the secondary pulmonary lobules alongside the bronchioles and venules in the walls of the lobules can also also produce this pattern in rare cases [1,2] when they are distended and distorted by tumor cells.

4. Discussion

4.1. Clinical discussion

A six-month course of fever, cough, and weight loss indicates a subacute process such as indolent infection, autoimmune disease, or malignancy. The pattern of lung nodules on this patient's chest CT included two distributions: a) branching centrilobular nodules most commonly associated with endobronchial spread of infection [2,3] and b) perilymphatic nodules situated in the walls of the secondary pulmonary lobules and along the pleural surface, a finding characteristic of sarcoidosis and lymphangitic malignancy. The combination of these two patterns can be seen in diffuse granulomatous infection such as tuberculosis and would have been consistent with the patient's symptoms. Thus, an extensive search for infection was undertaken but was unrevealing. Based on CT findings in isolation, sarcoidosis remained a possibility, but this condition alone would not have provided a unifying diagnosis. A clue leading in a different direction—that of malignancy—came from features concerning for HLH such as markedly elevated ferritin. The latest iteration of diagnostic guidelines for HLH was revised in 2004 and remains the most widely accepted (Table 1) [4]. According to these guidelines, clinicians are advised to consider HLH in adult patients with hyperferritinemia, especially concentrations >7000 μg/L. An elevated level of soluble IL-2 receptor further supports the diagnosis and has been recently shown to be a reliable marker of HLH with an area under the curve of 0.90(4). Up to 70% of adult HLH cases are associated with cancer, so this diagnosis should prompt a search

Table 1
Diagnostic criteria for Hemophagocytic Lymphohistiocytosis (HLH).

The diagnosis of HLH can be established if Criterion 1 or 2 is fulfilled.
1. A genetic molecular diagnosis consistent with HLH
2. Diagnostic criteria for HLH fulfilled (5 of the 8 criteria below)
Fever
Splenomegaly
Cytopenias (affecting ≥2 of 3 lineages in the peripheral blood)
Hemoglobin <90 g/L (hemoglobin <100 g/L in infants <4 wk)
Platelets <100 × 109/L
Neutrophils <1.0 × 109/L
Hypertriglyceridemia and/or hypofibrinogenemia
Fasting triglycerides ≥3.0 mmol/L (ie, ≥265 mg/dL)
Fibrinogen ≤1.5 g/L
Hemophagocytosis in bone marrow, spleen or lymph nodes. No evidence of malignancy.
Low or no NK cell activity (according to local laboratory reference)
Ferritin ≥500 μg/L (>3000 raises concern with most clinicians)
sCD25 (ie, soluble IL-2 receptor) ≥2400 U/mL

Adapted from Henter et al.[14]

for occult malignancy, especially a lymphoproliferative disorder. Certain types of lymphoma, among them IVLBCL, have a uniquely close association with HLH. The presence of cytopenias and profound LDH elevation in our patient pointed to a lymphoproliferative disorder as the unifying substrate for her symptoms and chest CT findings. After an unremarkable bone marrow biopsy, an alternative consideration became indolent fungal or viral infection. Bronchoscopy was thus performed for lung sampling in search of either as-yet undiscovered neoplasia or an elusive atypical infection. This procedure proved diagnostic. Once a diagnosis was established, the patient returned to the Dominican Republic to pursue treatment at a local institution. IVLBCL is known to be an aggressive disease, with a high score on the international prognostic index score [5]. Rituximab with anthracycline-based therapy(such as CHOP – Cyclophosphamide, doxorubicin, vincristine and prednisone) along with prophylactic CNS-directed therapy followed by consolidative Autologous stem cell transplantation may lead to long-term remission [5].

4.2. Radiologic discussion

The evaluation of micronodular disease at CT rests on identifying the distribution of nodules in the secondary pulmonary lobule, which is the smallest anatomic unit of the lung discernible at CT. Each of the three main patterns—random (hematogenous dissemination), perilymphatic, and centrilobular—is associated with a unique differential diagnosis. Perilymphatic distribution refers to nodules found in the expected locations of pulmonary lymphatics, namely along pleural surfaces, interlobular septa and bronchovascular bundles. Perilymphatic distribution suggests non-infectious granulomatous diseases such as sarcoidosis, and, less commonly, the granulomatous pneumoconioses such as silicosis and berylliosis. Lymphangitic carcinomatosis can also have this appearance, however, in most cases septal thickening predominates over nodularity, and the patient has a history of advanced malignancy.

Centrilobular distribution, also observed on our patient's chest CT, implies localization exclusively along the path of the bronchovascular bundle, which occupies the center of the secondary pulmonary lobule (Fig. 3A). By far the most common cause of this pattern is involvement of the bronchiolar compartment in the form of infection or inflammation. When the process underlying centrilobular nodularity leads to inspissated mucus or inflammatory exudate filling the bronchiolar lumina, these nodules acquire V- or Y-shapes, which correspond to the now visible arborizing bronchiolar network [6] (Fig. 3B). Bacterial, mycobacterial, and viral pathogens are the usual infectious culprits of bronchiolitis, whereas aspiration and allergic bronchopulmonary aspergillosis are examples of inflammatory causes. Because of bronchiolar obstruction, this pattern almost invariably is associated with air trapping, which manifests as increased lucency around the branching centrilobular nodules.

The other, much less common, source of centrilobular nodules is the arteriolar compartment. In this case, the conspicuous branching centrilobular nodules represent filling of the *vascular* lumina by solid material such as neoplastic cells. Another way by which metastatic malignancy can create this appearance is through carcinomatous endarteritis wherein fibrocellular intimal hyperplasia occurs as a reaction to tumor cells and obliterates the vascular lumen [1]. The nodules, in turn, correspond to discrete endovascular tumor deposits (Fig. 3C and D). Compared to bronchiolar disorders, their vascular counterpart may be more difficult to discern against the backdrop of normal branching vasculature [7], especially if the nodular component is small and ill-defined as is often the case.

In the largest published series, Cha and colleagues [8] described the CT characteristics of 11 patients with IVBCL involving the lungs. Ground glass opacities (GGO) were a near-ubiquitous finding among their cases; in contrast, GGO was not a prominent feature in the present case. Also reported were branching centrilobular nodules, corresponding histopathologically to vascular filling and perivascular extension by neoplastic cells, which was the preponderant finding in our patient. Cha and colleagues [8] propose that the "stalks" attached to the nodules and the peripheral branching tubular structures associated with nodules likely represent peripheral vessels that become engorged due to downstream obstruction to flow of blood by neoplastic cells (deposited as the nodule). In this regard, CT image reformatting using the maximal intensity projection (MIP) algorithm can facilitate detection and characterization of otherwise subtle micronodular findings [7]. Even if less subtle, given its rarity, attribution of centrilobular nodularity to vascular disease is likely to be overlooked as it was in this case. Of note, neoplasia is not the only etiology of this pattern; it has also been de-

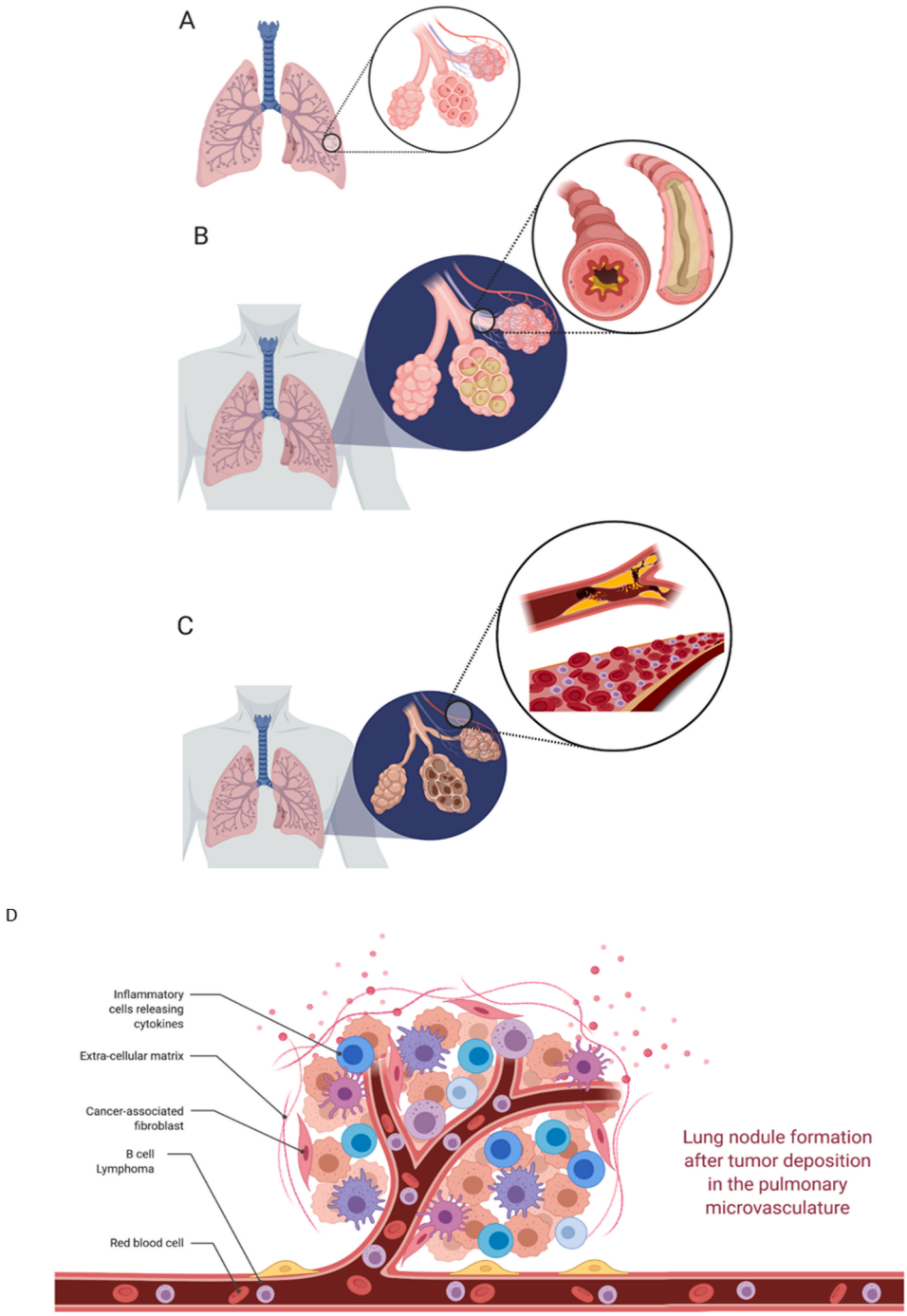

Fig. 3. A-B, Schematic representation of the normal tracheobronchial tree (panel A) ending with the terminal bronchiole, surrounded by pulmonary arterioles (red) and pulmonary venules (blue). Panel B represents bronchiolar causes of the centrilobular nodule pattern on chest CT, with edematous bronchial mucosa filled with inflammatory exudate (yellow). Panel C- Schematic representation of vascular causes of centrilobular nodules, with intraluminal tumor emboli/lymphoma cells (blue) resulting in centrilobular nodules associated with a feeding blood vessel. Panel D- Schematic representation of the microenvironment around the formation of the lung nodule caused by the deposition of intravascular tumor emboli or lymphoma cells.

Table 2
Summary of the immunohistochemical stains used in this case and their results.

Stain	Structure stained	Clinical significance	Patient result
CD20	B lymphocytes	This signifies a B cell lineage	Positive
CD34	Endothelial cells (and many other cells)	While serving as a positive internal control on tissues, it may help delineate intravascular pathology.	Positive
MUM1, (Multiple Myeloma 1)	B lymphocytes that arise from the germinal center of a lymph nodes	This helps divide diffuse large B cell lymphomas into germinal center (MUM1-; superior outcomes) and non-germinal center (post-germinal center or activated B-like, MUM1+) phenotypes	Positive
BCL-2 (B cell lymphoma-6)	B lymphocytes	This serves as an antiapoptotic protein	Positive
Anti Ki-67 antibody	Nuclear protein expressed in G1, S, G2 and M phases of cell cycle, absent in G0 phase	This serves as a marker of proliferation and "aggressiveness" of neoplastic cells.	(30–40% positive)
PAX5	Detected in Pro-B cells and mature B cells	More sensitive and specific than CD20 as a B cell marker	Positive
CD29	Diverse cell types, not expressed in IVLBCL	Involved in lymphocyte and endothelial adhesion; important for lymphocyte trafficking and transvascular migration	Negative
CD56	Marker of Natural Killer (NK) cells	Differentiates B cells (negative) from NK cells (positive)	Negative
CD3	Marker of T cells	Also called OKT3, may use as target for therapy with anti- CD3 Monoclonal antibodies	Negative
CD30	Lymphocyte activating antigen	Confirms diagnosis of classic Hodgkin's lymphoma, anaplastic large cell lymphoma, among others	Negative

scribed in association with so-called "excipient lung disease" wherein powdered foreign material is injected though intravenous catheters, resulting in granulomatous occlusion of pulmonary arterioles.

4.3. Pathologic discussion

IVLBCL is a rare form of extranodal LBCL characterized by selective growth of neoplastic cells within arterioles and capillaries. This malignancy was first described in 1959 by Pfleger and colleagues [9] and was thought to be an endothelial tumor before modern IHC techniques demonstrated the lymphoid origin of the neoplastic cells. In 2008, the World Health Organization officially categorized it as a subtype of extranodal diffuse LBCL. Exceptional cases of T and NK-cell intravascular lymphoma have been reported [10]. Besides being the location of uncontrolled cell division, blood vessels also serve as conduits for embolization throughout the body with commonly involved sites being the central nervous system, skin, and lung; lymph nodes are typically spared. The inability of these tumor cells to express adhesion molecules, such as CD29, and matrix metalloproteinases has been proposed as the reason they cannot traverse the vascular space [11]. A complex tumor micro-environment (Fig. 3D) exists in organs where the neoplastic cells proliferate [12], with each component representing a target for future therapeutic strategies. Some inflammatory cells that have been described as important constituents of this local inflammatory milieu include tumor macrophages, dendritic cells, T lymphocytes and NK cells, with the purpose of causing neoplastic cell apoptosis, through PD-1/PD-L1 and other pathways [12], while extracellular matrix proteins recruited to support cellular interactions and limit the spread of disease [13].

IVLBCL is an aggressive and highly lethal lymphoma that is notorious for evading antemortem diagnosis and being discovered only at autopsy. The neoplastic lymphoid cells found on this patient's transbronchial lung biopsy were large with a high nucleus/cytoplasm ratio, irregular nuclear contours, and open chromatin (Fig. 2A and B). The distribution pattern of these cells inside blood vessels was discohesive (i.e., free-floating), best appreciated on the CD34 immunostain, which is specific for endothelial cells and so helps create contrast with the negatively stained lymphoid cells (Fig. 2C). The lymphoid cells stained positively for CD20, confirming their B-cell lineage (Fig. 2D and E). Also positive were the BCL-6 and MUM-1 immunostains, indicating a non-germinal center origin of the lymphoma (not shown). The Ki-67 index was 30–40%, a marker of the aggressive nature of this neoplasm. A summary of the immunohistochemical staining results of this patient's lymphoma appears in Table 2. Taken together, the morphological and immunohistochemical pattern of the lung biopsy tissue is consistent with LBCL, favoring intravascular type. A major competing diagnosis for this entity is DLBCL not otherwise specified and, indeed, they share many immunohistochemical properties. Fluorescence in-situ hybridization did not demonstrate CMYC rearrangement, BCL2-IGH gene rearrangement, or BCL6 (3927) breakpoint translocation—a cytogenetic profile typical of IVLBCL.

5. Conclusions

HLH is strongly associated with underlying malignancy and may be the sentinel sign of a heretofore undetected lymphoproliferative disorder. If the standard investigation for lymphoma fails to identify its presence, a close look at the appearance of the lung parenchyma on chest CT is warranted to exclude subtle signs of branching centrilobular nodularity as a potential indicator of lymphoma hiding within blood vessels. Recognition of this CT finding in our patient prompted lung biopsy, which yielded the classically challenging diagnosis of IVLBCL and unified all of the features of her presentation. Contemporary advances in thoracic imaging and immunohistochemical staining have made IVLBCL an increasingly realistic antemortem diagnosis [14].

CRediT authorship contribution statement

Ravi Manglani: Writing – review & editing, Writing – original draft, Software, Resources, Data curation, Conceptualization. **Ji-Hae Shin:** Writing – original draft, Conceptualization. **Venkata Sireesha Chemarthi:** Writing – original draft, Conceptualization. **Mohamad Raji:** Software, Resources. **Anna Rozenshtein:** Writing – review & editing, Supervision, Conceptualization. **Oleg Epelbaum:** Writing – review & editing, Writing – original draft, Supervision, Conceptualization.

Declaration of competing interest

The authors declare that they have no known competing financial interests or personal relationships that could have appeared to influence the work reported in this paper.

References

[1] N. Bhalla, C.-F. Chang, C. Lee, Special considerations for tree-in-bud nodules, Annals of the American Thoracic Society 16 (5) (2019) 636–638.
[2] E. Terhalle, G. Günther, 'Tree-in-Bud': thinking beyond infectious causes, Respiration 89 (2) (2015) 162–165.
[3] W.T. Miller Jr, J.S. Panosian, Causes and imaging patterns of tree-in-bud opacities, Chest 144 (6) (2013) 1883–1892.
[4] P. La Rosée, A. Horne, M. Hines, T. von Bahr Greenwood, R. Machowicz, N. Berliner, et al., Recommendations for the management of hemophagocytic lymphohistiocytosis in adults, Blood 133 (23) (2019) 2465–2477.
[5] A. Mukherjee, I.F. Ibrahim, Intravascular large B-cell lymphoma: an elusive diagnosis with challenging management, J Community Support Oncol 16 (6) (2018) e280–e282.
[6] N. Verma, J.H. Chung, T.-L.H. Mohammed, Tree-in-Bud sign, J. Thorac. Imag. 27 (2) (2012).
[7] A. Devakonda, S. Raoof, A. Sung, W.D. Travis, D. Naidich, Bronchiolar disorders: a clinical-radiological diagnostic algorithm, Chest 137 (4) (2010) 938–951.
[8] M.J. Cha, K.S. Lee, H.S. Hwang, T.J. Kim, T.S. Kim, B.-T. Kim, et al., Pulmonary intravascular lymphomatosis: clinical, CT, and PET findings, correlation of CT and pathologic results, and survival outcome, Radiology 280 (2) (2016) 602–610.
[9] J. Tappeiner, L. Pfleger, [Angioendotheliomatosis proliferans systematisata. A clinically and pathohistologically new disease picture], Hautarzt 14 (1963) 67–70.
[10] L. Cerroni, C. Massone, H. Kutzner, T. Mentzel, P. Umbert, H. Kerl, Intravascular large T-cell or NK-cell lymphoma: a rare variant of intravascular large cell lymphoma with frequent cytotoxic phenotype and association with Epstein-Barr virus infection, Am. J. Surg. Pathol. 32 (6) (2008) 891–898.
[11] M. Ponzoni, E. Campo, S. Nakamura, Intravascular large B-cell lymphoma: a chameleon with multiple faces and many masks, Blood 132 (15) (2018) 1561–1567.
[12] R. Tamma, G. Ranieri, G. Ingravallo, T. Annese, A. Oranger, F. Gaudio, et al., Inflammatory cells in diffuse large B cell lymphoma, J. Clin. Med. 9 (8) (2020) 2418.
[13] A.I. Cioroianu, P.I. Stinga, L. Sticlaru, M.D. Cioplea, L. Nichita, C. Popp, et al., Tumor microenvironment in diffuse large B-cell lymphoma: role and prognosis, Anal. Cell Pathol. 2019 (2019) 8586354.
[14] V. Brunet, S. Marouan, J.P. Routy, M.A. Hashem, V. Bernier, R. Simard, et al., Retrospective study of intravascular large B-cell lymphoma cases diagnosed in Quebec: a retrospective study of 29 case reports, Medicine (Baltim.) 96 (5) (2017) e5985.